The HIV-1 gp41 N-Terminal Heptad Repeat Plays an Essential Role in Membrane Fusion

Kelly Sackett and Yechiel Shai*,‡

Department of Biological Chemistry, Weizmann Institute of Science, Rehovot 76100, Israel

Received January 9, 2002; Revised Manuscript Received February 7, 2002

ABSTRACT: For many different enveloped viruses the crystal structure of the fusion protein core has been established. A striking conservation in the tertiary and quaternary arrangement of these core structures is repeatedly revealed among members of diverse families. It has been proposed that the primary role of the core involves structural rearrangements which facilitate apposition between viral and target cell membranes. Forming the internal trimeric coiled coil of the core, the N-terminal heptad repeat (NHR) of HIV-1 gp41 was suggested to have additional roles, due to its ability to bind biological membranes. The NHR is adjacent to the N-terminal hydrophobic fusion peptide (FP), which alone can fuse biological membranes. To investigate the role of the NHR in membrane fusion, we synthesized and functionally characterized HIV-1 gp41 peptides corresponding to the FP and NHR alone, as well as continuous peptides made of both FP and NHR (wild type and mutant). We show here that a consecutive, 70-residue peptide consisting of both the FP and NHR (gp41/1−70) has dramatic fusogenic properties. The effect of including the complete NHR, as compared to shorter 23-, 33-, or 52-residue N-terminal peptides, is illustrated by a leap in lipid mixing of phosphatidylcholine (PC) large unilamellar vesicles (LUV) and clearly delineates the synergistic role of the NHR in the fusion event. Furthermore, a mutation in the NHR that renders the virus noninfectious is reflected by a significant reduction in in vitro lipid mixing induced by the mutant, gp41/1−70 (I62D). Additional spectroscopic studies, characterizing membrane binding and apposition induced by the peptides, help to clarify the role of the NHR in membrane fusion.

Enveloped viruses need to fuse with the plasma membrane of target cells in order to deposit their genomic information, thereby catalyzing a new cycle of infection. This fusion event is believed to be carried out by virally encoded envelope glycoproteins (ENV's), termed fusion proteins. Expressed as oligomers on the surface of infected cells, viral fusion proteins are highly concentrated in the viral envelope, which is formed by budding from infected cell membranes. In the case of HIV-1,[1] the fusion protein is expressed as a polypeptide precursor, gp160, that is endoproteolytically cleaved to generate the transmembrane (TM) subunit, gp41, and the surface (SU) subunit, gp120 (*1*). gp41/gp120 remain noncovalently associated (*2*) and are trimeric in their native, prefusogenic state (*3*). The two subunits act as a tag team to initiate viral infection. Target cell specificity and binding are the responsibility of gp120, which first binds to the CD4 receptor (*4*−*6*) and then to one of a group of chemokine receptors (*7*−*9*). Receptor-induced conformational changes in gp120 allow the gp41 subunit to effect the merging of viral and target cell membranes (*10*, *11*).

Studied extensively, the gp41 subunit is made of an approximately 175-residue ectodomain, a single pass TM domain, and an approximately 150-residue endodomain. Much of the data gathered on gp41 comes from the study of peptide fragments from the ectodomain, which can be further reduced to three main functional subdomains: fusion peptide (FP), N-terminal heptad repeat (NHR), and C-terminal heptad repeat (CHR) (Figure 1). N-Terminal fragments from the FP region insert into membranes (*12*−*16*) and single handedly induce aggregation (*16*, *17*) and lipid mixing of model membrane vesicles (*14*, *16*−*18*). Extension of the FP to include the adjacent 10 aa polar region (FP analogue) increases the fusogenic function to the extent where fusion is observed in a highly stringent system, employing LUV composed of PC as the sole phospholipid (*19*). Site-directed mutagenesis in the FP region, demonstrating reduction or loss of function in vivo (*20*, *21*), corroborates with an analogous change in vesicle fusion activity for the corresponding FP analogue mutant (*19*, *22*). Crystallographic studies of peptide fragments from the NHR and CHR show that the NHR forms a trimeric coiled coil, providing a hydrophobic interface for three CHR peptides to pack as α-helices in an antiparallel arrangement (*23*−*25*). This core structure is believed to represent the final low-energy fusion conformation due to its high thermostability (*26*), while the native state of ENV is altered by elevated temperatures (*27*). Amino acid sequence analysis of 862 HIV-1 isolates from

* To whom correspondence should be addressed. Tel: 972-8-9342711. Fax: 972-8-9344112. E-mail: Yechiel.Shai@ weizmann.ac.il.

‡ The Harold S. and Harriet B. Brady Professorial Chair in Cancer Research.

[1] Abbreviations: BOC, butyloxycarbonyl; FMOC, 9-fluorenylmethoxycarbonyl; FP, fusion peptide; NHR, N-terminal heptad repeat; CHR, C-terminal heptad repeat; HF, hydrogen fluoride; HIV, human immunodeficiency virus; LUV, large unilamellar vesicles; MESNA, 2-mercaptoethanesulfonic acid; NBD-F, 4-fluoro-7-nitrobenz-2-oxa-1,3-diazole; PAM, phenylacetamidomethyl; PBS, phosphate-buffered saline; PC, egg phosphatidylcholine; PE, phosphatidylethanolamine; RP-HPLC, reverse-phase high-performance liquid chromatography; Rho, tetramethylrhodamine; SUV, small unilamellar vesicles; TES, triethylsilane.

10.1021/bi0255322 CCC: $22.00
Published on Web 03/12/2002

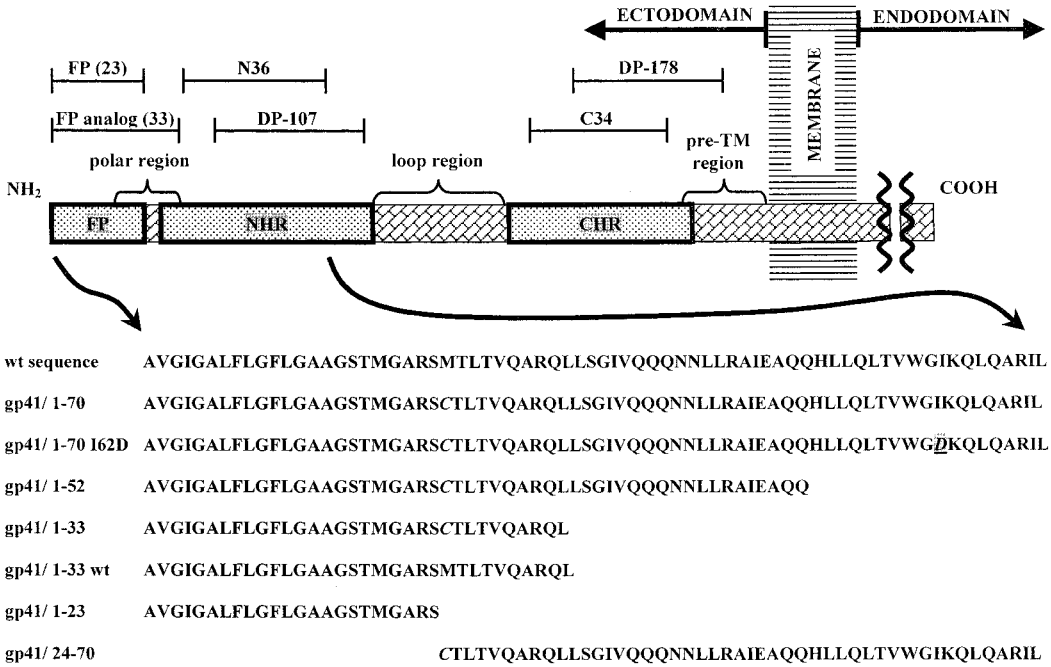

FIGURE 1: Schematic of the HIV-1 gp41 primary structure in scale. Primary functional subdomains are dotted and outlined, with additionally characterized regions specified by a brace. Above and in brackets are peptide fragments that have been extensively studied and will be referred to throughout the text. The number in parentheses refers to the length of the N-terminal FP. Below are peptides represented in this study, which correspond to the N-terminal wild-type sequence as indicated. The M24C mutation is italicized to emphasize placement of a cysteine residue for the purpose of ligating peptide fragments (see Materials and Methods section).

varying clades demonstrates greater than 97% conservation for residues that are involved in maintaining the coiled-coil structure, as well as those involved in forming the hydrophobic corridor for packing of CHR helices (*23*, *28*). Nonconservative mutations in the leucine/isoleucine backbone of the NHR abrogate viral infectivity, though expression, oligomerization, and localization of the fusion protein complexes remain unaffected (*29*−*31*). The NHR is also believed to be involved directly in membrane perturbation since peptides from this region exhibit binding to model membranes (*32*−*34*).

To address the involvement of the NHR in the membrane fusion event, we employed a native chemical ligation strategy (*35*) to extend the 23-residue FP C-terminally. By ligating to the FP, consecutive peptides of different lengths (mutant or wt), we generated the following N-terminal constructs: (i) gp41/1−33, (ii) gp41/1−52, (iii) gp41/1−70, and (iv) gp41/1−70 (I62D) (Figure 1). This latter peptide harbors a nonconservative mutation in the leucine/isoleucine backbone of the NHR at a position 62 residues from the N-terminus, which destabilizes the secondary structure and decreases membrane binding affinity of the NHR peptide DP-107 (*34*) (see Figure 1), as well as abrogates viral infectivity (*30*). The ligation products, along with nonligated fragments, were assayed for their ability to induce lipid mixing and apposition of model membranes comprised of PC LUV. Fluorescently labeled analogues were used to compare membrane partitioning to the same vesicles. Our results demonstrate that the NHR is primarily involved in merging of membranes and works synergistically with the FP to dramatically boost lipid mixing. Furthermore, a significant reduction in lipid mixing induced by the mutant gp41/1−70 (I62D) corresponds to in vivo loss of function by the same mutation (*30*).

MATERIALS AND METHODS

Materials. BOC and F-MOC amino acids, BOC-methylbenzhydrylamine resin, and F-MOC methylbenzhydrylamine resin (Rink Amide) were purchased from Nova-biochem AG (Laufelfingen, Switzerland). *S*-Trityl-β-mercaptopropionic acid was purchased from Peptides International (Louisville, KY). Other reagents for peptide synthesis, egg phosphatidylcholine (PC), and the sodium salt of 2-mercaptoethanesulfonic acid (MESNA) were purchased from Sigma. *N*-(Lissamine rhodamine B-sulfonyl)dioleoylphosphatidylethanolamine (Rho-PE), *N*-(7-nitrobenz-2-oxa-1,3-diazol-4-yl)dioleoylphosphatidylethanolamine (NBD-PE), and NBD fluoride (NBD-F) were purchased from Molecular Probes (Eugene, OR). All other reagents were of analytical grade. Buffers were prepared using doubly glass-distilled water. Phosphate-buffered saline (PBS) is composed of NaCl (8 g/L), KCl (0.2 g/L), KH_2PO_4 (0.2 g/L), and Na_2HPO_4 (1.09 g/L), at pH 7.3.

Peptide Synthesis and Fluorescent Labeling. The 23-residue N-terminal "linker peptide" was synthesized by a manual solid-phase method on methylbenzhydrylamine resin using BOC chemistry as previously described (*36*, *37*), with modifications outlined by Hackeng et al. (*35*), required for inclusion of the linker moiety (*S*-trityl-β-mercaptopropionic acid). Labeling of the N-terminus of this peptide with NBD-F was achieved as previously described (*38*, *39*). BOC peptides were cleaved from the resin by HF. All other peptides were synthesized by a F-MOC solid-phase method on Rink Amide methylbenzhydrylamine resin, using an ABI 433A automatic peptide synthesizer, and then cleaved from the resin using a cocktail made of TFA/DDW/TES [18.5:1:0.5 (v/v)]. All peptides were purified by RP-HPLC on a C4 Bio-Rad semipreparative column to >98% homogeneity, and the mass

of each peptide was confirmed by platform LCA electrospray mass spectrometry.

Native Chemical Ligation. The ligation of unprotected fragments was carried out as described (*35*) with the following alterations: (1) We used MESNA as the catalyst (*40*). (2) Prior to addition of lyophilized peptides, the pH of the reaction mixture, made of 5.5 M GnCl, 0.1 M Na_2HPO_4, and 1% MESNA (w/v), was adjusted to ~7.2 using 1 M NaOH. (3) Ligations were carried out at peptide concentrations ranging from 0.1 to 0.8 mM. (4) The various ligations were incubated over a range of temperatures, from 4 to 37 °C, and for a period of 4−5 days. For each ligation, the product resolved as a single isolated peak and was purified to >98% homogeneity using RP-HPLC. Product identity was confirmed by mass spectrometry.

Amidation of the "Linker" Peptide. To generate the 23-residue FP fragment, amidated at the C-terminus, a molar excess of NH_3 was added to the linker peptide solubilized in 50% AcN. RP-HPLC was used to follow the reaction and to purify the product to >98% homogeneity. An amide group effectively replaced the linker and leucine group at the C-terminus as evidenced by the appearance of a new peak with a peptide-like spectrum (the conjugated linker moiety induces a specific spectrum), as well as mass confirmation using mass spectrometry. Unless stated elsewhere, stock solutions of concentrated peptide in DMSO with a 10-fold molar excess of DTT were used to deliver the peptides into aqueous or lipidic solutions to avoid aggregation and disulfide dimerization of the peptides prior to use.

Preparation of Large Unilamellar Vesicles (LUV). PC was dissolved in a 2:1 (v/v) mixture of chloroform/methanol and then dried under a stream of nitrogen gas while rotating, thereby depositing a thin film of PC on the wall of a glass vial. Excess solvent was removed by overnight lyophilization. Dry lipids were suspended in PBS buffer by vortexing to produce large multilamellar vesicles. The lipid suspension was freeze−thawed 6 times and then extruded 20 times through polycarbonate membranes with 0.1 μm diameter pores (Nuclear Corp., Pleasanton, CA) to generate LUV.

Peptide-Induced Lipid Mixing. Lipid mixing of LUV was measured using a fluorescence probe dilution assay (*41*). PC LUV containing 0.6 molar % each of NBD-PE as the energy donor and Rho-PE as the energy acceptor were prepared in PBS as described above. A 1:4 mixture of labeled and unlabeled vesicles (110 μM total phospholipid concentration) was suspended in 400 μL of PBS, and a small volume of peptide in stock solution was added. The increase in NBD fluorescence at 530 nm (8 nm slit) was monitored, with the excitation set at 467 nm (8 nm slit). The fluorescence intensity before the addition of the peptide was referred to as 0% lipid mixing, and the fluorescence intensity upon addition of reduced Triton X-100 [0.05% (v/v)] was referred to as 100% lipid mixing. All fluorescence measurements were done on an SLM-AMINCO Bowman series 2 luminescence spectrometer.

Electron Microscopy. The effects of the peptides on liposome suspensions were determined by negative stain electron microscopy. Prior to staining and fixing, suspensions of PC LUV at 4.5 mM (with or without lyophilized peptide) were incubated for 5 min at room temperature. A drop of the suspension containing PC LUV or a mixture of PC LUV and peptide at a peptide/lipid molar ratio of 0.01 was deposited onto a carbon-coated grid and negatively stained with phosphotungstic acid (2%, pH 6.8). The grids were examined using a JEOL JEM 100B electron microscope (Japan Electron Optics Laboratory Co., Tokyo, Japan).

Membrane Binding Experiments. The degree of peptide association with PC LUV was determined using NBD-labeled peptides. The sensitivity of the NBD moiety to the dielectric constant of its surroundings allows for the determination of the environment of the NBD-labeled peptides. It has been shown previously that the fluorescence emission of NBD increases and shifts to lower wavelengths (blue shift) upon relocation of the NBD moiety to a more hydrophobic environment (*38*, *42*). The changes in fluorescence intensity were measured following addition of increasing amounts of LUV to 0.1 μM NBD-labeled peptides until a plateau had been reached (after subtracting the contribution of the vesicles alone). The fluorescence intensity was measured as a function of the lipid/peptide molar ratio, with the excitation set at 467 nm (8 nm slit) and the emission set at 530 nm (8 nm slit).

Visible Absorbance Measurements. Changes in the size of vesicles were measured by visible absorbance. Aliquots of peptide stock solutions were added to 200 μL suspensions of 90 μM PC LUV in PBS. Absorbance was measured at 405 nm using a Bio-Tek Instruments microplate reader before and after the addition of peptide.

RESULTS

Experimental System. Represented in this study are synthetic peptide fragments from the N-terminal half of the gp41 ectodomain (Figure 1). To overcome difficulties in the synthesis of the long peptides, we employed a "native chemical ligation strategy" (*35*), whereby the N-terminal 23-residue linker peptide (with a linker moiety attached at its C-terminus) was ligated to continuous fragments of different lengths (all containing a cysteine at their N-terminus, required for ligation). A native peptide bond seals the ligation seam. Because the region of gp41 under study lacks a cysteine, we decided to mutate methionine at position 24 for the following reasons: (i) position 24 tolerates variation (*28*), and (ii) a break at this position facilitates generation and comparison of peptides corresponding to the well-characterized FP and the NHR region.

Regarding the membrane mimetic environment, we chose LUV composed solely of PC since this is a major outer leaflet phospholipid in both target cell and viral membranes and additionally mimics the zwitterionic nature of the same biological surfaces. With respect to model membrane systems, PC LUV are difficult to fuse and therefore represent a highly stringent membrane to test fusogenic function. It is known that inclusion of components such as PE or negatively charged lipids into liposomes creates vesicles more facile to fusion (*14*, *43*).

The Cysteine Mutation (M24C) Affords No Loss of Fusogenic Function. The effect of the M24C mutation on the fusogenic function was tested by comparing the lipid mixing ability of the wild-type FP analogue (gp41/1−33 wt) to its corresponding M24C mutant (gp41/1−33). In Figure 3A, the data confirm the fusogenic ability of the fusion peptide analogue (gp41/1−33 wt) (*19*, *22*, *44*). Furthermore, the ability of gp41/1−33 wt to induce lipid mixing is not

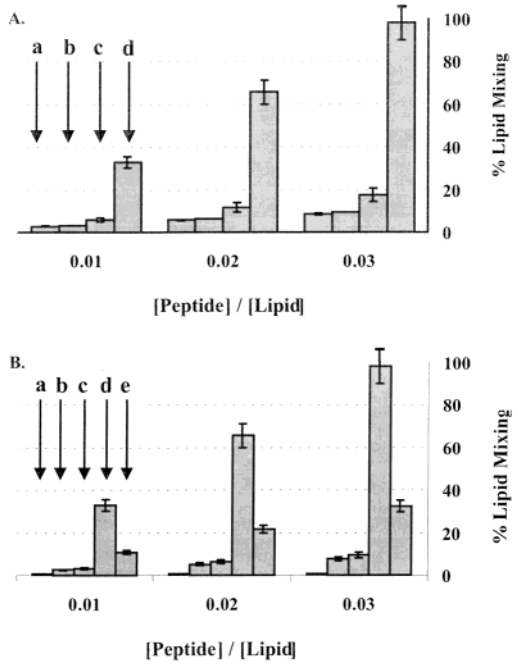

FIGURE 2: Dose dependence of lipid mixing of PC LUV induced by the peptides. In separate experiments, increasing amounts of peptide were added to a fixed amount of vesicles. The maximal values of the fluorescence intensity, following addition of peptide, were plotted as a function of the peptide/lipid molar ratio. For all peptides, we observed a linear correlation between the percent lipid mixing and the peptide/lipid molar ratio, with the corresponding percent error illustrated with brackets representing a linear average of two to three individual experiments. A linear fit function was used to define the linear correlation of the dose−response curves for individual experiments, with R^2 values ranging from 0.970 to 0.998. For precision, the data set used to establish the linear fit extended to 0.08 peptide/lipid for all peptides except gp41/1−70 and gp41/1−70 (I62D). Panel A: (a) gp41/1−33, (b) gp41/1−33 wt, (c) gp41/1−52, and (d) gp41/1−70. Panel B: (a) gp41/1−23, (b) gp41/24−70, (c) gp41/1−23 + 24−70, equimolar mixture, (d) gp41/1−70, and (e) gp41/1−70 (I62D).

compromised by inclusion of the cysteine mutation [gp41/1−33 (M24C)]. These two peptides are equal in their ability to mix membranes of PC LUV. The M24C mutation is required for the ligation chemistry to extend the fusion peptide C-terminally, and therefore all extended peptides retain the M24C mutation.

Inclusion of the Complete NHR Boosts Fusion Ability Dramatically. Illustrated in Figure 3A is a clear relationship between the length of the N-terminal gp41 fragment and its effectiveness at fusing PC LUV. We confirm earlier findings that the FP (gp41/1−23) is unable to fuse PC vesicles over the concentration range tested (*13*, *16*). The gp41/1−52 peptide, which extends to include approximately one-half of the NHR, is approximately twice as fusogenic as the shorter gp41/1−33 constructs. Remarkably, the gp41/1−70 peptide, which extends to include all of the NHR [as defined by extensive protease digestion (*45*)], is 10 times as active as the fusion peptide analogue gp41/1−33 and five times more active than the gp41/1−52 fragment. These results suggest a novel role for the NHR: specifically, direct involvement in mediating membrane fusion.

The FP/NHR Composite Is Responsible for the Fusion Activity of the Ectodomain. A peptide from an additional region in the HIV-1 gp41 ectodomain, namely, the pretransmembrane region (see Figure 1), has been reported to have

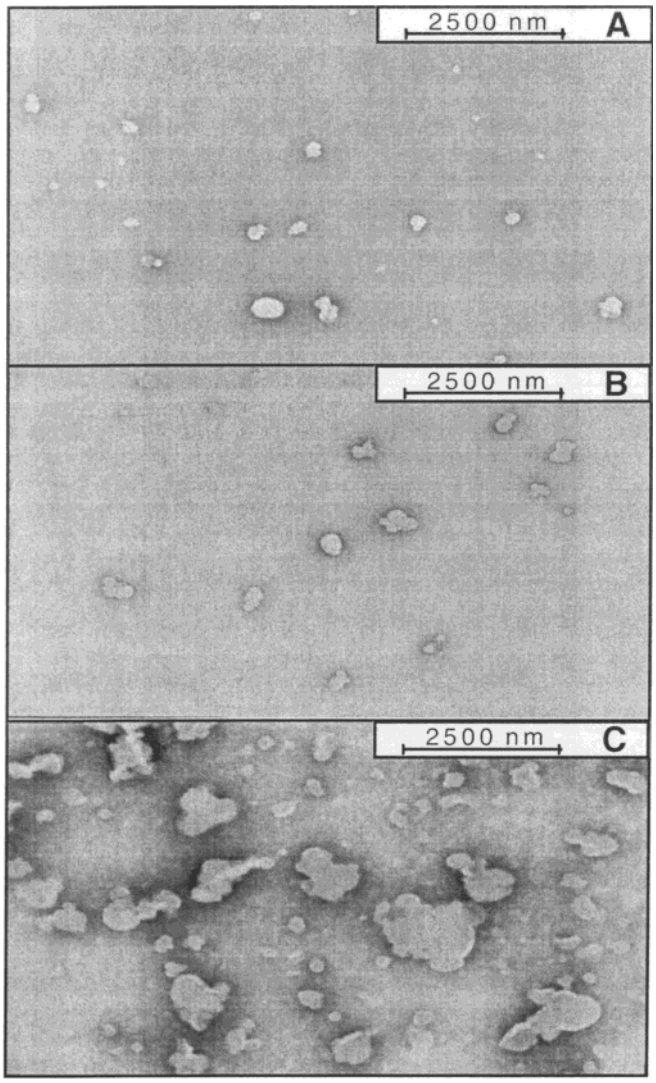

FIGURE 3: Electron micrographs confirm fusion. Shown are micrographs of negatively stained PC LUV (4.5 mM) in the absence and presence of different peptides at a 0.01 peptide/lipid molar ratio. Panels: (A) PC LUV alone; (B) PC LUV incubated with gp41/1−23; (C) PC LUV incubated with gp41/1−70.

fusogenic properties (*46*). This region is comparable to the 23-residue FP in inducing lipid mixing (J. L. Nieva, personal communication). This latter result substantiates the HIV gp41 FP/NHR composite as being primarily involved in the membrane fusion event. On the basis of previous biochemical studies, the FP was implicated as being the main mediator of viral fusion (*16*, *17*). The striking difference between the fusogenic potency of the FP and the FP/NHR composite indicates that the FP/NHR composite is responsible for bearing the bulk of the membrane fusion work.

The NHR Region (gp41/24−70) Is a Fusogenic Fragment. We report here a novel fusogenic sequence from the HIV-1 gp41 ectodomain. Comparing panels A and B of Figure 3, we see that gp41/24−70 can induce lipid mixing of PC LUV as effectively as the FP analogue, gp41/1−33. The NHR region was implicated to be involved in membrane fusion, since mutations in this region depress or abolish gp41-mediated fusion (*29*−*31*, *47*). Furthermore, peptide fragments from this gp41/24−70 NHR region adopt α-helical, coiled-coil structures in solution (*23*, *26*, *32*, *34*, *48*−*50*) and bind to the surface of membranes as α-helices (*33*, *34*). The fact

that gp41/24−70 is fusogenic on its own, combined with the markedly enhanced fusion observed in the FP/NHR composite (gp41/1−70), further confirms the novel fusogenic role of NHR region.

The FP and NHR Regions Act Synergistically When Conjugated. Given the clear lipid mixing effect of gp41/24−70, contrasted with the nonfunctional gp41/1−23, we show that equimolar mixtures of the FP and the NHR region (gp41/24−70) are only slightly more effective than gp41/24−70 alone. Significantly, the continuous FP/NHR composite (gp41/1−70) is substantially more fusogenic than either the FP or NHR region alone or as a mixture (Figure 3B). Our results demonstrate the synergy played between the FP and the NHR regions of HIV-1 gp41 in mediating membrane fusion.

A Loss of Function Mutation in Vivo Correlates with Significantly Reduced Function in Vitro. The gp41/1−70 (I573D) peptide harbors a mutation in the "a" position of the leucine/isoleucine zipper backbone of the NHR, located far from the N-terminal fusion peptide. Well characterized, this mutation significantly reduces the secondary α-helical structure of the DP-107 peptide (see Figure 1) in solution (*34*) and is a loss of function mutation in vivo despite proper expression, localization, and oligomerization of native fusion protein complexes (*30*). Our results show that gp41/1−70 (I62D) is significantly less fusogenic than its gp41/1−70 counterpart (Figure 3B). This finding validates the biological relevance of our model system and further supports the direct involvement of the NHR in the actual fusion step.

Electron Microscopy Confirms Membrane Fusion. To confirm that the observed lipid mixing (see Figure 2) is indeed a function of vesicle fusion, we utilized negative stain electron microscopy to visualize PC LUV before and after incubation with peptide. Shown in Figure 3 are representative micrographs of PC LUV alone (panel A), PC LUV incubated with gp41/1−23 (panel B), and PC LUV incubated with gp41/1−70 (panel C). The micrographs corroborate the lipid mixing results previously described. Specifically, while gp41/1−70 causes a substantial increase in vesicle size, gp41/1−23 induces no change in vesicle size. These results confirm that the lipid mixing induced by gp41/1−70 is a result of membrane fusion.

The Peptides Bind Similarly to Membranes. To determine whether the observed variation in fusogenic character was due to differential membrane binding of the peptides, we N-terminally labeled the following peptides with NBD to determine their membrane binding character: gp41/1−33, gp41/1−52, gp41/1−70, and its mutant gp41/1−70 (I62D). A fixed amount of labeled peptide was titrated with increasing amounts of PC LUV, and the increase in fluorescence intensity due to membrane partitioning was recorded as a function of the lipid/peptide molar ratio. The resultant binding curves are shown in Figure 4. Since the peptides oligomerize in aqueous solution, their binding curves were not analyzed further. The binding curves all reached saturation at lipid/peptide molar ratios similar to what has been observed previously for NBD labeled gp41/1−33 wt (*19*, *22*, *44*). Comparison to soluble antimicrobial peptides with similar saturation points suggests that the three peptides share a partition coefficient on the order of 10^4 M^{-1} (*39*, *51*). The similar membrane binding character of the peptides assayed cannot explain their range of variation with respect to fusion.

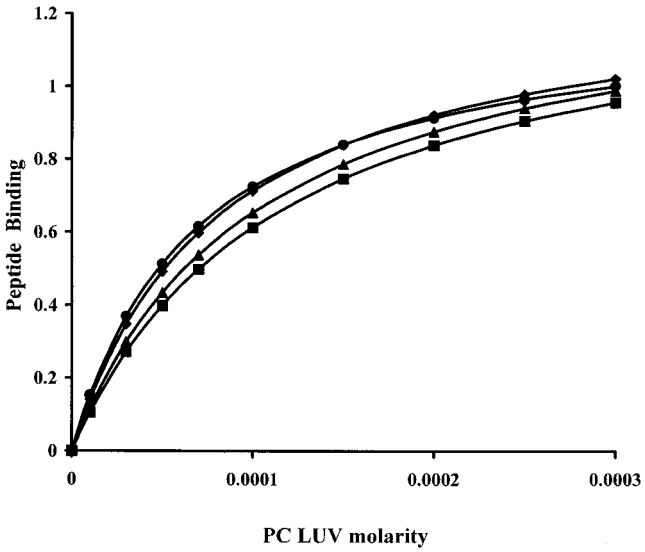

FIGURE 4: Membrane binding affinity of the peptides. The following binding isotherms are based on the increase in the fluorescence of NBD-labeled peptides (0.1 μM) upon titration with PC LUV. Titrations were performed at room temperature in PBS. The excitation wavelength was set at 467 nm (8 nm slit) and emission recorded at 530 nm (8 nm slit). Key: (●) gp41/1−33 NBD, (◆) gp41/1−70 NBD, (▲) gp41/1−70 (I62D) NBD, and (■) gp41/1−52 NBD.

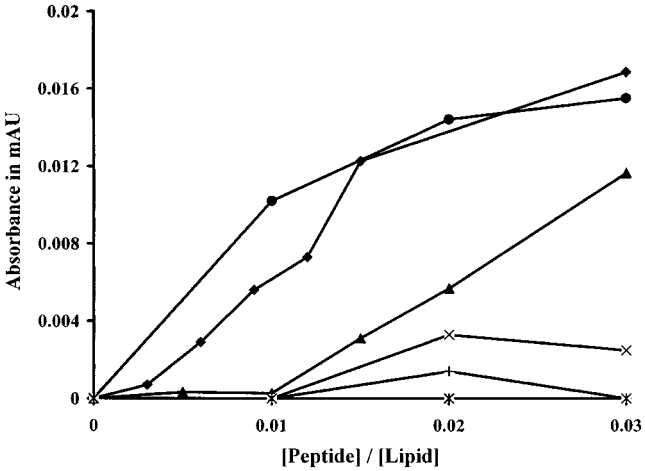

FIGURE 5: Light scattering induced by the peptides. Detection of aggregation and/or fusion is followed by measuring absorbance changes at 405 nm of PC LUV mixed with peptides. Peptides were added to 90 μM PC LUV in PBS. The changes in absorbance at 405 nm, as measured in milli-absorption units (mAU), are plotted versus the peptide/lipid molar ratio. Key: (◆) gp41/1−70, (●) gp41/1−33, (▲) gp41/1−70)I62D), (×) gp41/24−70, (+) gp41/1−23, and (*) gp41/1−23 + 24−70, equimolar mixture.

Induction of Vesicle Aggregation by the Peptides. Membrane apposition is a necessary step before membrane fusion can occur. The ability of the peptides to induce vesicle aggregation was tested in order to investigate whether this property is responsible for the differences in their ability to fuse membranes. Changes in vesicle size distribution resulting from peptide-induced aggregation and/or fusion can be monitored by following the absorbance of the liposome suspension. The changes in absorbance at 405 nm of PC LUV as a function of the peptide/lipid molar ratio are shown in Figure 5. The data reveal that the difference in fusogenic potency between gp41/1−33 and 1−70 is not a function of their respective ability to increase light absorbance of the

LUV suspension. For the following peptides, we see a stepwise gradation in their ability to increase light absorbance, which corresponds to their respective fusogenic potencies: gp41/1−70, gp41/1−70 (I62D), gp41/24−70, and gp41/1−23. In contrast, the equimolar mixture of gp41/1−23 and 24−70 and gp41 1−52 (not shown) cause no change in light absorbance. Additionally, gp41/1−33 wt is equal to gp41/1−33 at increasing light absorbance (not shown).

DISCUSSION

Fusion of phospholipid vesicles is believed to involve three major steps: vesicle aggregation, membrane destabilization, and merging of the two membranes (*43*, *52*−*54*). Using a stringent model membrane system (PC LUV), we assayed the fusogenic character of HIV-1 gp41 peptides corresponding to the N-terminal half of the ectodomain. We show here that the NHR is essentially involved in membrane fusion.

The mechanism by which gp41 causes membrane fusion is poorly understood, though evidence has been accumulated in support of models describing the fusion event. A prevailing model describes gp41 as existing in at least two states: metastable and stable. In unbound, native gp41/120, the gp41 subunits are in a metastable state that is maintained by association with gp120 subunits (*10*, *23*). Following receptor binding, gp120 undergoes conformational changes, thereby freeing gp41 to form an extended, α-helical rodlike conformation that translocates the FP outward, facilitating its insertion into the target cell membrane (*55*, *56*). This "prehairpin" conformation exposes the NHR and CHR regions, which remain vulnerable to the inhibitory activities of peptide inhibitors up to 15 min following initial receptor−ENV interactions (*57*). Peptide inhibitors derived from heptad repeat regions of the ectodomain are thought to act by binding to their counterparts in gp41, mimicking the structural organization involved in forming the core. Active at nanomolar concentrations, DP-178 (see Figure 1) is derived from the CHR and binds to the corresponding NHR (*26*, *58*, *59*) but has also been shown to bind to the FP region (*60*, *61*). Viruses resistant to DP-178 have mutations that map to residues in the NHR region (*62*). In the absence of inhibitors, the NHR and CHR regions are believed to draw together, apposing the two tethered membranes, and fold into the low-energy '"hairpin" or core conformation. The energy liberated as a result of folding into the highly thermostable core structure is believed to help offset the energy involved in merging of the opposing membranes (*26*).

The profound effect of the NHR in mediating vesicle fusion implies an essential role during viral ENV-mediated fusion. Membrane fusion is an energy-costing event since it involves destabilization of the bilayers and dehydration of the interface regions of merging membranes (*63*). The NHR region can bind to and destabilize membranes throughout the fusion event, exerting its effects at two levels: (1) protein−lipid interactions and (2) protein−protein interactions (intra- and intermolecular). Shortly after insertion of the FP into the target cell membrane, N-terminal regions of the NHR can act to destabilize membranes. This assertion is validated by Piesajovich et al. (*44*), showing that the polar region (see Figure 1) has membrane-perturbing effects, which is confirmed by our results comparing the fusogenic potency of the FP to the FP analogue (Figure 2). Subsequent membrane apposition can be driven by the low solubility of the NHR region (*45*) and its ability to bind membranes (*32*−*34*) and oligomerize (*56*, *64*, *65*). Membrane destabilization to the point of hemifusion can be characterized structurally by the formation of stalk-like intermediates (*43*, *66*), which provide a scaffold for facile binding of the extended coiled coil [see illustrations in Bentz (*67*)]. Binding and membrane destabilization at this point are likely given the fusogenic effects of gp41/24−70, as well as the fact that DP-178 effectively inhibits viral fusion at latter stages (*57*) and can act on membrane bound targets (*33*). At the level of protein−protein interactions, the tendency of the NHR to oligomerize into a trimeric coiled coil would localize FP's inserted in the cell membrane, thereby initiating fusion pore formation. The NHR may also induce or stabilize the structure in the FP region. This is likely since the NHR has been shown to induce the secondary structure of adjacent C-terminal regions in the ectodomain (*23*−*26*, *59*, *68*), as well as induce oligomerization of otherwise monomeric proteins fused to its N-terminus (*69*, *70*).

Early studies predicted that the coiled-coil structure adjacent to the N-terminal FP is a common theme in viral fusion protein architecture (*71*). The fusogenic interplay between these two subdomains is consistent among different viral families. The HA2 and F-protein subunits of influenza and Sendai virus fusion proteins, respectively, correspond to the gp41 subunit of the HIV fusion protein. The NHR of F-protein has been shown to bind membranes (*72*, *73*), as does that of gp41 (*32*−*34*). Ghosh and Shai showed that the NHR acts synergistically with the FP in inducing membrane fusion for the Sendai F-protein (*74*). Compared to gp41 and HA2, the F-protein has a much larger ectodomain with a FP that is only mildly fusogenic (*75*), implying that additional regions are involved in mediating fusion. By analogy, the FP of HA2 is mildly fusogenic (*76*−*78*), while extension to include most of the NHR generates a peptide with far greater fusogenic potency (*79*). Our results demonstrating the fusogenic potential of the FP/NHR composite of gp41 further support the idea of a common fusion mechanism among various enveloped viruses. Crystallographic and biochemical structural analyses demonstrate the ordering of specific subdomains within the ectodomain, with formation of a conserved structural core motif among different families of enveloped viruses (*10*, *23*, *26*, *32*, *80*−*82*). Collectively, these results support the suggestion advanced by Weissenhorn et al. (*10*) that positioning of coiled coils parallel to the surface of two opposing membranes, while maintaining physical linkage between the membranes via insertion of FP into target membrane and TM anchoring to viral membrane, may represent a common fusion intermediate essential to the mechanism of viral-induced membrane fusion.

ACKNOWLEDGMENT

We are grateful to Dr. Y. Marikovsky for help in visualizing phospholipid vesicles using electron microscopy and to S. G. Peisajovich for counsel.

REFERENCES

1. Freed, E. O., and Martin, M. A. (1995) *J. Biol. Chem. 270*, 23883−23886.
2. Veronese, F. D., DeVico, A. L., Copeland, T. D., Oroszlan, S., Gallo, R. C., and Sarngadharan, M. G. (1985) *Science 229*, 1402−1405.

3. Zhang, C. W., Chishti, Y., Hussey, R. E., and Reinherz, E. L. (2001) *J. Biol. Chem. 276*, 39577−39585.
4. Maddon, P. J., Dalgleish, A. G., McDougal, J. S., Clapham, P. R., Weiss, R. A., and Axel, R. (1986) *Cell 47*, 333−348.
5. McDougal, J. S., Maddon, P. J., Dalgleish, A. G., Clapham, P. R., Littman, D. R., Godfrey, M., Maddon, D. E., Chess, L., Weiss, R. A., and Axel, R. (1986) *Cold Spring Harbor Symp. Quant. Biol. 51*, 703−711.
6. Dalgleish, A. G., Beverley, P. C., Clapham, P. R., Crawford, D. H., Greaves, M. F., and Weiss, R. A. (1984) *Nature 312*, 763−767.
7. Feng, Y., Broder, C. C., Kennedy, P. E., and Berger, E. A. (1996) *Science 272*, 872−877.
8. Jones, P. L., Korte, T., and Blumenthal, R. (1998) *J. Biol. Chem. 273*, 404−409.
9. Alkhatib, G., Combadiere, C., Broder, C. C., Feng, Y., Kennedy, P. E., Murphy, P. M., and Berger, E. A. (1996) *Science 272*, 1955−1958.
10. Weissenhorn, W., Dessen, A., Calder, L. J., Harrison, S. C., Skehel, J. J., and Wiley, D. C. (1999) *Mol. Membr. Biol. 16*, 3−9.
11. Wyatt, R., and Sodroski, J. (1998) *Science 280*, 1884−1888.
12. Chang, D. K., Cheng, S. F., and Chien, W. J. (1997) *J. Virol. 71*, 6593−6602.
13. Curtain, C., Separovic, F., Nielsen, K., Craik, D., Zhong, Y., and Kirkpatrick, A. (1999) *Eur. Biophys. J. 28*, 427−436.
14. Martin, I., Defrise-Quertain, F., Decroly, E., Vandenbranden, M., Brasseur, R., and Ruysschaert, J. M. (1993) *Biochim. Biophys. Acta 1145*, 124−133.
15. Pereira, F. B., Goni, F. M., Muga, A., and Nieva, J. L. (1997) *Biophys. J. 73*, 1977−1986.
16. Rafalski, M., Lear, J. D., and DeGrado, W. F. (1990) *Biochemistry 29*, 7917−7922.
17. Nieva, J. L., Nir, S., Muga, A., Goni, F. M., and Wilschut, J. (1994) *Biochemistry 33*, 3201−3209.
18. Pereira, F. B., Goni, F. M., and Nieva, J. L. (1995) *FEBS Lett. 362*, 243−246.
19. Pritsker, M., Rucker, J., Hoffman, T. L., Doms, R. W., and Shai, Y. (1999) *Biochemistry 38*, 11359−11371.
20. Delahunty, M. D., Rhee, I., Freed, E. O., and Bonifacino, J. S. (1996) *Virology 218*, 94−102.
21. Freed, E. O., Myers, D. J., and Risser, R. (1990) *Proc. Natl. Acad. Sci. U.S.A. 87*, 4650−4654.
22. Kliger, Y., Aharoni, A., Rapaport, D., Jones, P., Blumenthal, R., and Shai, Y. (1997) *J. Biol. Chem. 272*, 13496−13505.
23. Chan, D. C., Fass, D., Berger, J. M., and Kim, P. S. (1997) *Cell 89*, 263−273.
24. Tan, K., Liu, J., Wang, J., Shen, S., and Lu, M. (1997) *Proc. Natl. Acad. Sci. U.S.A. 94*, 12303−12308.
25. Weissenhorn, W., Dessen, A., Harrison, S. C., Skehel, J. J., and Wiley, D. C. (1997) *Nature 387*, 426−430.
26. Lu, M., Blacklow, S. C., and Kim, P. S. (1995) *Nat. Struct. Biol. 2*, 1075−1082.
27. Moore, J. P., and Klasse, P. J. (1992) *AIDS Res. Hum. Retroviruses 8*, 443−450.
28. Dong, X. N., Xiao, Y., Dierich, M. P., and Chen, Y. H. (2001) *Immunol. Lett. 75*, 215−220.
29. Chen, S. S., Lee, C. N., Lee, W. R., McIntosh, K., and Lee, T. H. (1993) *J. Virol. 67*, 3615−3619.
30. Dubay, J. W., Roberts, S. J., Brody, B., and Hunter, E. (1992) *J. Virol. 66*, 4748−4756.
31. Wild, C., Dubay, J. W., Greenwell, T., Baird, T., Jr., Oas, T. G., McDanal, C., Hunter, E., and Matthews, T. (1994) *Proc. Natl. Acad. Sci. U.S.A. 91*, 12676−12680.
32. Kliger, Y., Peisajovich, S. G., Blumenthal, R., and Shai, Y. (2000) *J. Mol. Biol. 301*, 905−914.
33. Kliger, Y., Gallo, S. A., Peisajovich, S. G., Munoz-Barroso, I., Avkin, S., Blumenthal, R., and Shai, Y. (2001) *J. Biol. Chem. 276*, 1391−1397.
34. Rabenstein, M., and Shin, Y. K. (1995) *Biochemistry 34*, 13390−13397.
35. Hackeng, T. M., Griffin, J. H., and Dawson, P. E. (1999) *Proc. Natl. Acad. Sci. U.S.A. 96*, 10068−10073.
36. Merrifield, R. B., Vizioli, L. D., and Boman, H. G. (1982) *Biochemistry 21*, 5020−5031.
37. Shai, Y., Bach, D., and Yanovsky, A. (1990) *J. Biol. Chem. 265*, 20202−20209.
38. Rapaport, D., and Shai, Y. (1991) *J. Biol. Chem. 266*, 23769−23775.
39. Rapaport, D., and Shai, Y. (1992) *J. Biol. Chem. 267*, 6502−6509.
40. Evans, T. C., Jr., Benner, J., and Xu, M. Q. (1998) *Protein Sci. 7*, 2256−2264.
41. Struck, D. K., Hoekstra, D., and Pagano, R. E. (1981) *Biochemistry 20*, 4093−4099.
42. Rajarathnam, K., Hochman, J., Schindler, M., and Ferguson-Miller, S. (1989) *Biochemistry 28*, 3168−3176.
43. Chernomordik, L., Kozlov, M. M., and Zimmerberg, J. (1995) *J. Membr. Biol. 146*, 1−14.
44. Peisajovich, S. G., Epand, R. F., Pritsker, M., Shai, Y., and Epand, R. M. (2000) *Biochemistry 39*, 1826−1833.
45. Lu, M., and Kim, P. S. (1997) *J. Biomol. Struct. Dyn. 15*, 465−471.
46. Suarez, T., Nir, S., Goni, F. M., Saez-Cirion, A., and Nieva, J. L. (2000) *FEBS Lett. 477*, 145−149.
47. Chen, S. S. (1994) *J. Virol. 68*, 2002−2010.
48. Lawless, M. K., Barney, S., Guthrie, K. I., Bucy, T. B., Petteway, S. R., and Merutka, G. (1996) *Biochemistry 35*, 13697−13708.
49. Kliger, Y., and Shai, Y. (2000) *J. Mol. Biol. 295*, 163−168.
50. Wild, C., Oas, T., McDanal, C., Bolognesi, D., and Matthews, T. (1992) *Proc. Natl. Acad. Sci. U.S.A. 89*, 10537−10541.
51. Pouny, Y., Rapaport, D., Mor, A., Nicolas, P., and Shai, Y. (1992) *Biochemistry 31*, 12416−12423.
52. Blumenthal, R. (1987) *Curr. Top. Membr. Transp. 29*, 203−254.
53. Lucy, J. (1982) *Biological Membranes*, Academic Press, London.
54. Nir, S., Bentz, J., and Wilschut, J. (1980) *Biochemistry 19*, 6030−6036.
55. Furuta, R. A., Wild, C. T., Weng, Y., and Weiss, C. D. (1998) *Nat. Struct. Biol. 5*, 276−279.
56. Weissenhorn, W., Wharton, S. A., Calder, L. J., Earl, P. L., Moss, B., Aliprandis, E., Skehel, J. J., and Wiley, D. C. (1996) *EMBO J. 15*, 1507−1514.
57. Munoz-Barroso, I., Durell, S., Sakaguchi, K., Appella, E., and Blumenthal, R. (1998) *J. Cell Biol. 140*, 315−323.
58. Wild, C. T., Shugars, D. C., Greenwell, T. K., McDanal, C. B., and Matthews, T. J. (1994) *Proc. Natl. Acad. Sci. U.S.A. 91*, 9770−9774.
59. Wild, C., Greenwell, T., Shugars, D., Rimsky-Clarke, L., and Matthews, T. (1995) *AIDS Res. Hum. Retroviruses 11*, 323−325.
60. Neurath, A. R., Strick, N., and Jiang, S. (1992) *Virology 188*, 1−13.
61. Neurath, A. R., Lin, K., Strick, N., and Jiang, S. (1995) *AIDS Res. Hum. Retroviruses 11*, 189−190.
62. Rimsky, L. T., Shugars, D. C., and Matthews, T. J. (1998) *J. Virol. 72*, 986−993.
63. Rand, R. P. (1981) *Annu. Rev. Biophys. Bioeng. 10*, 277−314.
64. Shu, W., Ji, H., and Lu, M. (1999) *Biochemistry 38*, 5378−5385.
65. Poumbourios, P., Wilson, K. A., Center, R. J., El Ahmar, W., and Kemp, B. E. (1997) *J. Virol. 71*, 2041−2049.
66. Markin, V. S., Kozlov, M. M., and Borovjagin, V. L. (1984) *Gen. Physiol. Biophys. 5*, 361−377.
67. Bentz, J. (2000) *Byophis. J. 78*, 886−900.
68. Kliger, Y., and Shai, Y. (2000) *J. Mol. Biol. 295*, 163−168.
69. Shugars, D. C., Wild, C. T., Greenwell, T. K., and Matthews, T. J. (1996) *J. Virol. 70*, 2982−2991.

70. Bernstein, H. B., Tucker, S. P., Kar, S. R., McPherson, S. A., McPherson, D. T., Dubay, J. W., Lebowitz, J., Compans, R. W., and Hunter, E. (1995) *J. Virol. 69*, 2745−2750.
71. Chambers, P., Pringle, C. R., and Easton, A. J. (1990) *J. Gen. Virol. 71*, 3075−3080.
72. Ben-Efraim, I., Kliger, Y., Hermesh, C., and Shai, Y. (1999) *J. Mol. Biol. 285*, 609−625.
73. Ghosh, J. K., Peisajovich, S. G., Ovadia, M., and Shai, Y. (1998) *J. Biol. Chem. 273*, 27182−27190.
74. Ghosh, J. K., and Shai, Y. (1999) *J. Mol. Biol. 292*, 531−546.
75. Rapaport, D., and Shai, Y. (1994) *J. Biol. Chem. 269*, 15124−15131.
76. Lear, J. D., and DeGrado, W. F. (1987) *J. Biol. Chem. 262*, 6500−6505.
77. Rafalski, M., Ortiz, A., Rockwell, A., van Ginkel, L. C., Lear, J. D., DeGrado, W. F., and Wilschut, J. (1991) *Biochemistry 30*, 10211−10220.
78. Epand, R. F., Macosko, J. C., Russell, C. J., Shin, Y. K., and Epand, R. M. (1999) *J. Mol. Biol. 286*, 489−503.
79. LeDuc, D. L., Shin, Y. K., Epand, R. F., and Epand, R. M. (2000) *Biochemistry 39*, 2733−2739.
80. Lamb, R. A., Joshi, S. B., and Dutch, R. E. (1999) *Mol. Membr. Biol. 16*, 11−19.
81. Bullough, P. A., Hughson, F. M., Skehel, J. J., and Wiley, D. C. (1994) *Nature 371*, 37−43.
82. Yang, Z. N., Mueser, T. C., Kaufman, J., Stahl, S. J., Wingfield, P. T., and Hyde, C. C. (1999) *J. Struct. Biol. 126*, 131−144.

BI0255322